RSC Advances

PAPER

View Article Online
View Journal | View Issue

Cite this: *RSC Adv.*, 2024, **14**, 4880

Design of gum Arabic/gelatin composite microcapsules and their cosmetic applications in encapsulating tea tree essential oil

Wei Yang,[ab] Yuxi Gong,[a] Yansong Wang,[a] Chao Wu,[a] Xiangyu Zhang,*[ab] Jinlian Li*[ab] and Dongmei Wu *[ab]

Microencapsulation has been widely used to protect essential oils, facilitating their application in cosmetics. In this study, gelatin, gum arabic and *n*-butyl cyanoacrylate were used as wall materials, and composite microcapsules of tea tree essential oil (TTO) were prepared using a combination of composite coagulation and *in situ* polymerization methods. When the ratio of gelatin to gum arabic is 1 : 1, the ratio of TTO to *n*-butyl cyanoacrylate is 4 : 1, the curing time is 10 h, and the encapsulation efficiency (EE) under these conditions is 73.61%. Morphological observation showed that the composite capsule was a micron-sized spherical particle with an average particle size of 10.51 μm, and Fourier transform infrared spectroscopy (FT-IR) confirmed a complex coagulation reaction between gelatin and gum arabic, and the disappearance of the *n*-butyl cyanoacrylate peak indicated that the film was formed in a condensation layer. The thermogravimetric analysis (TGA) results showed that the composite capsule greatly improved the thermal stability of TTO. Rheological testing showed that the viscosity and viscoelasticity of the surface composite capsules have been improved. In addition, the composite capsule showed good stability in the osmotic environment and has good sustained-release performance and antioxidant capacity in the average human skin environment.

Received 13th December 2023
Accepted 18th January 2024

DOI: 10.1039/d3ra08526k

rsc.li/rsc-advances

1 Introduction

Developing composite materials with controlled structures and specific properties is currently a challenge in many technological and industrial fields.[1–3] TTO is widely used for its whitening and antioxidant properties. However, its application is limited owing to its sensitivity to light, heat, pH, and other conditions.[4,5] Therefore, we need a carrier to protect TTO and overcome the limitations of TTO application. Microcapsules are tiny particles formed with polymer wall materials coating core materials, which are solids, liquids and gases. Microencapsulation can effectively reduce the damage caused by harsh peripheral environment to the core materials of volatile small molecules and protect, stabilize, and prolong the service life and release rate of core materials.[6,7] As a result, TTO encapsulated in microcapsules are widely used in food and cosmetics.[8–10]

Owing to their low cost, compatibility, excellent thermal stability and controllable preparation process, polymers are often used as shell materials for microencapsulating essential oils. Polymer shell materials can determine the properties of microcapsules, including their morphology, size distribution and structure.[11] Gelatin and gum arabic are commonly used materials in the complex coacervation method. Coacervate capsules prepared by this method exhibit excellent biocompatibility, surface activity and high encapsulation efficiency.[12–15] Studies have confirmed that as carriers for protection and delivery, individual complex coacervation capsules lack stability in harsh solution conditions. Dardelle *et al.*[16] confirmed that composite capsules improve the stability of capsules against diffusion loss compared to simple gel capsules.

It is confirmed that compared with traditional microcapsules with a single shell structure, composite microcapsules prepared by combining various preparation methods can combine the advantages of different shell structures, thus effectively improving the pressure resistance and thermal stability of microcapsules[17] and compensating for the shortcomings of a single shell and enhancing the performance of microcapsules through additional shell layers.[18–20] The composite coacervation method and the *in situ* polymerization method are commonly used preparation methods for microcapsules. Complex coacervation is a coacervation process between two or more polymers.[21] *In situ* polymerization is a technology of mixing reactive monomers with core materials and controlling polymer deposition at the interface by adjusting pH and temperature to form dense films.[22,23] We referred to the modification polymerization method of cyanide acrylic ester.[24]

[a]*College of Pharmacy, Jiamusi University, Jiamusi, Heilongjiang 154007, P. R. China. E-mail: zhangxy@jmsu.edu.cn; lijinlian@jmsu.edu.cn; dmwu@jmsu.edu.cn*
[b]*Heilongjiang Provincial Key Laboratory of New Drug Development and Pharmacotoxicological Evaluation, Jiamusi University, Jiamusi 154007, P. R. China*

Opt for introducing cyanopropyl acrylic acid *n*-butyl ester and combining complex coacervation and *in situ* polymerization to prepare composite capsules of TTO. Cyanopropyl acrylic acid *n*-butyl ester, as a medical adhesive, has the advantages of low toxicity, good film-forming properties,[25] and ease of operation, enhancing the sustained release capability and stability of microcapsules in permeable environments.

This study used gelatin, gum arabic, and butyl cyanoacrylate as shell materials and combined coacervation and *in situ* polymerization methods to encapsulate TTO, resulting in composite TTO microcapsules. The microcapsules' particle size distribution, morphology, and EE were characterized. Finally, the stability, release behavior, and antioxidant capacity of the modified microcapsules were investigated.

2 Materials and methods

2.1 Materials

TTO (laboratory extraction). Gelatin (bloom: 100, isoelectric point: 4.72), gum arabic, sodium hydroxide (NaOH), and glacial acetic acid were purchased from Sinopharm Group Chemical Reagent Co. *N*-Butyl-cyanoacrylate was purchased from the Chongqing Jingu Rubber Industry. DPPH and ABTS were purchased from Shanghai Yuan Ye Biotechnology Co. In addition to TTO, all reagents used in this experiment were of analytical grade and used as received unless stated otherwise. Triple distilled water was used throughout the investigation.

2.2 Preparation of TTO/gum Arabic/gelatin composite microcapsules

We used the improved aggregation method developed by B. Fasipe *et al.*[20] to prepare composite microcapsules. 10 mL of 2% gelatin solution was mixed with gum arabic solution at 40 °C, and stirred well with the acetic acid solution and the pH was adjusted to 4.0. Then, 0.11 g of butyl cyanoacrylate was combined with 0.5 g of tea tree oil and dripped into the gelatin and gum arabic solution. The solution was stirred for 2 hours, cooled with cold water, followed by addition of glutamine transferase, and solidified for 10 h. After preparation, the sample was washed several times with purified water to eliminate the impurities and placed in a freeze-dryer to obtain a freeze-dried microcapsule powder sample for further analysis.

2.3 Drug loading capacity and EE

According to the test method of Liu *et al.*,[17] the packaging efficiency is calculated, and some modifications are done. The freeze-dried powder sample (0.5 g) was combined with 30 mL ethanol at 40 °C for 5 min without destroying microcapsules, and the beaker was gently shaken to extract surface TTO. The freeze-dried powder sample (0.5 g) was mixed with 30 mL of ethanol and sonicated for 20 min to completely break down the microcapsules, followed by centrifugation at 1000 rpm for 20 min. After extraction, we collected the supernatant of both. The ultraviolet absorption value determines the amount of surface oil and total oil at 265 nm, and the standard curve is drawn by the TTO–ethanol common solution prepared in advance, and its equation is $y = 0.73071C + 0.00831$ ($R^2 = 0.99914$). Then, EE is obtained by eqn (1).[26] The equation is as follows:

$$\mathrm{EE} = \frac{\text{total oil} - \text{surface oil}}{\text{total oil}} \times 100\% \quad (1)$$

2.4 Characteristic analysis of compound capsules

A small amount of microcapsule powder was gently sprayed on the conductive adhesive, the excess powder on the surface was blown off with an ear-washing ball, and then gold was sprayed on the sample and it was observed under a scanning electron microscope (JBM-7800F).

A Baxter laser particle size analyzer (Baxter 90 nanometer particle size analyzer) was used to determine the size distribution of microcapsules.

The potassium bromide particle method was used to conduct the infrared spectrum experiment of microcapsules. The microcapsule powder and potassium bromide sample crystals are mixed, evenly ground, and compressed to prepare samples. A Fourier transform infrared spectrometer (VERTEX 70) measured the transmission infrared spectrum. The scanning range is 4000–500 cm^{-1}.

A thermogravimetric analyzer (STA 449C) was utilized to test the thermal stability of microcapsules. The sample was heated from 30 °C to 600 °C at a rate of 10 °C min^{-1} under a nitrogen atmosphere.

2.5 Rheological property determination

Using a dynamic rheometer (HR10 US) at 25 °C, the viscosity was measured at shear rates ranging from 0.01 to 100 s^{-1}. At the same temperature, the viscoelasticity of the microcapsules was measured within the linear viscoelastic range at frequencies from 100 to 0.1 rad.

2.6 Volatile compound analysis

Gas chromatography-mass spectrometry refers to the method of Liu *et al.*[17] Using a gas chromatography-mass spectrometry (GC9790II) instrument for the analysis of TTO and TTO complex capsules, the following conditions were applied: HP-5 column, injector temperature of 250 °C, and detector temperature of 250 °C. The initial column temperature was maintained at 80 °C for 1 min, then increased at a rate of 10 °C min^{-1} to 120 °C and held for 3 min, followed by an increase at a rate of 15 °C min^{-1} to 230 °C and held for 2 min. The sample volume was 0.5 mL, with a split ratio of 50 : 1, and a carrier gas flow rate of 1 mL min^{-1}.

2.7 Stability study

The new TTO condensed capsules and TTO composite capsules were put in a specific concentration of sodium dodecyl sulfate solution to simulate the stability of the capsules in a relatively harsh environment with permeability. The micro-morphology of microcapsules was observed initially and after soaking for

15 h, and the concentration of TTO in the solution was measured *via* UV-vis spectrophotometry every 3 h to reflect the stability of condensed capsules and composite capsules in an osmotic environment.

2.8 *In vitro* release studies of composite microcapsules

Sustained release performance is a significant index to evaluate the quality of microcapsules. We studied and compared the release behaviour of condensed and composite capsules at room temperature. The microcapsules were positioned in an open environment at 37 °C, pH 5.5, and the same amount of samples were collected at regular intervals (3, 6, 9, 12 and 15 days). The content of TTO in the microcapsules was detected by UV-vis spectrophotometry. The release amount of TTO was calculated, and the curve of the release amount of essential oil with time was obtained.

2.9 Determination of antioxidant properties

Sample Preparation: a certain amount (based on the mass of TTO) of TTO, TTO microencapsulated powder, and TTO composite capsule powder was weighed out. Each was dissolved in an equal volume of anhydrous ethanol to ensure that the concentration of TTO is identical in all three solutions.

Sample solution (2 mL) was extracted from each of the above samples at a specific time interval, gently shaken and centrifuged to form a clear sample solution. The 2,2-diphenyl-1-picrylhydrazyl (DPPH) and 2,2-azinobis(3-ethylbenzothiazoline-6-sulfonic acid ammonium salt) (ABTS) scavenging rates were measured under the conditions of human skin (37 °C, pH 5.5).

2.9.1 Determination of DPPH scavenging rate. We used the procedure of A. J. Cheruth *et al.*[27] and made some modifications to determine the DPPH clearance rate. Firstly, 2 mL of DPPH ethanol solution was centrifuged and 2 mL of anhydrous ethanol was added, and then 2 mL of DPPH ethanol solution was centrifuged and 2 mL of TTO ethanol solution, condensed capsule powder solution and composite capsule powder solution was added, respectively. The solution was shaken well, mixed vigorously, and left to react in the dark for 30 min, and the absorbance of each mixed solution was identified at 517 nm by enzyme immunoassay. The calculation of DPPH scavenging rate is based on formula (2):[28]

$$\text{DPPH radical scavenging rate} = \frac{A_0 - A}{A_0} \times 100\% \quad (2)$$

where A_0 is the absorbance of 2 mL of DPPH–ethanol and 2 mL of 10% ethanol; A is the absorbance of 2 mL of ethanol and 2 mL of sample solution.

2.9.2 Determination of ABTS scavenging rate. P. A. Loyeau *et al.*'s[29] method with slight modifications was referred to determine the ABTS scavenging rate. A certain amount of ABTS solution was mixed with a certain amount of $K_2S_2O_8$ solution. The sample was left in the dark overnight, and diluted with anhydrous ethanol before measurement to ensure an absorption peak at 734 nm.

First, 2 mL of ABTS ethanol solution was centrifuged and 2 mL of anhydrous ethanol was added. Then, another 2 mL of ABTS ethanol solution was centrifuged and 2 mL each of TTO ethanol solution, coagulant capsule powder solution, and composite capsule powder solution was added. The solution was mixed well, vigorously shaken, and left to react in the dark for 30 minutes. The enzyme immunoassay was used to determine the absorbance of each mixed solution at 734 nm. The calculation of ABTS clearance rate is based on formula (3):[30]

$$\text{ABTS radical scavenging rate} = 1 - \frac{A_1 - A_2}{A_3} \times 100\% \quad (3)$$

where A_1 is the absorption of 2 mL sample solution and 2 mL ABTS stock solution; A_2 is the absorbance of 2 mL sample solution and 2 mL 95% ethanol; A_3 is the absorbance of 2 mL ABTS stock solution and 2 mL 10% ethanol.

3 Results and discussion

3.1 The schematic illustration of the fabrication of composite microcapsules

The preparation and formation of micro-capsules are illustrated in Fig. 1. Gelatin and gum arabic are dissolved in water, respectively, to constitute a solution. When gelatin and gum arabic are completely dissolved, the two solutions are mixed. Acidic dissolution is in addition to adjusting the pH to make the adhesive tape positively charged. The adhesive tape reacts with the negatively charged gum arabic in a complex coagulation reaction in the solution, and liquid–liquid separation occurs through electrostatic interaction. In this process, van der Waals force and hydrophobic interaction in protein will further promote the formation of complex condensation.[31] Cyanoacrylate will spontaneously undergo a rapid polymerization reaction under the action of nucleophiles. When the TO combined with *n*-butyl cyanoacrylate is added to the gelatin–gum arabic mixed solution, cyanoacrylate will rapidly polymerize due to contact with water, forming a polycyanoacrylate film. By stirring, the film is wrapped by the condensed layer.[32] Finally, a bilayer microcapsule with a coagulation layer on the outside and *n*-butyl cyanoacrylate on the inside is formed.

3.2 Optimization of preparation conditions

3.2.1 Effect of the dosage of TTO and *n*-butyl α-cyanoacrylate on EE. Fig. 2(a) illustrates the relationship between the ratio of TTO to *n*-butyl cyanoacrylate and the EE. The encapsulation of composite capsules first increased and then decreased. When the ratio of TTO to *n*-butyl cyanoacrylate is 4 : 1, the EE is the highest, reaching 72.26%. The polymerization rate of α-butyl cyanoacrylate is very fast after it is compounded with water.[33,34] In the case of low doses, *n*-butyl cyanoacrylate can be consumed during the formation of composite capsules. With the increase in dosage, the *n*-butyl cyanoacrylate may not be wholly consumed, which leads to excessive *n*-butyl cyanoacrylate polymerization to form irregular polymers, which destroys the formed composite capsules and affects the formation of new capsules so that the EE will decrease.

3.2.2 Effect of dosage ratio of gelatin to gum Arabic on EE. Fig. 2(b) illustrates the relationship between the mass ratio of

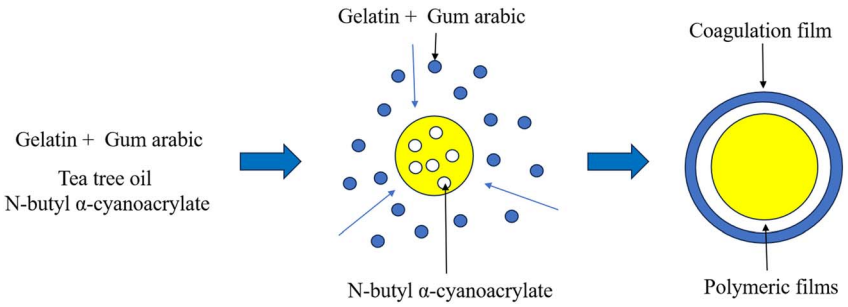

Fig. 1 Schematic diagram of preparation of composite microcapsules.

gelatin to gum arabic and the EE. Because the dosage ratio of gelatin to gum arabic is different, it can be seen from the figure that the encapsulation first rises and then falls; when the ratio of gelatin to gum arabic is 1 : 1, the EE is the highest, reaching 71.93% and the increase of gelatin content in the system leads to the rise of composite coagulant, forming a more stable coagulation layer. When the amount of gelatin exceeds that of gum arabic, the EE of microcapsules decreases gradually. The reason may be that positively charged gelatin remains in the aqueous solution, which destroys the formation of capsules. Therefore, when the mass ratio of gelatin to gum arabic is 1 : 1,[35] the packaging efficiency is the highest, which is the best mass ratio of gelatin to gum arabic.

3.2.3 Effect of curing time on EE. Fig. 2(c) illustrates the relationship between curing time and packaging efficiency. With the increase in curing time, the EE also increased gradually, and the highest EE was 73.1% at 10 h. When the curing time continued to increase, the EE decreased slightly. Glutamine transaminase catalyzes the polymerization and cross-linking of protein molecules by catalyzing the covalent bond between lysine and glutamic acid of gelatin molecules.[36] The curing process of microcapsules is slow, and with the extension of curing time, the structure of the condensed layer will be more stable. When the curing time is short, the condensed layer is unstable, and it is easy to break in the subsequent operation, resulting in the leakage of TTO. When the curing time reaches 10 h, the curing effect reaches the best state,[37] the microcapsule structure is stable and not easy to destroy, and the packaging efficiency is the highest. Therefore, 10 h is selected as the best curing time for microcapsules.

3.2.4 Optimizing compound capsules using response surface methodology. In order to statistically evaluate the model, it is necessary to conduct an analysis of variance. A p-value <0.05 is considered significant for the relationship between the independent and dependent variables. The model's p-value of 0.0001 < 0.05 indicates a good effect. Furthermore, $R^2 = 0.979$ further confirms the excellent fit of the model. The regression equation between three factors (the mass ratio of gelatin to gum arabic A, the mass ratio of TTO to cyanopropyl acrylate butyl ester B, and the curing time C) and the response variable (EE) is as follows: $EE = 73.528 - 0.576A - 0.276B + 1.88C - 0.285AB + 0.4225AC + 0.493BC - 3.809A^2 - 5.439B^2 - 3C^2$. The EE range of the composite capsule is 55.2% to 73.4%. The three factors have a significant impact on EE. The mass ratio of gelatin to gum arabic affects the charge in the solution and is crucial for the formation of the coacervate layer. The mass ratio of TTO to cyanopropyl acrylate butyl ester affects the core material content and the formation of the polymer film. The curing time determines whether the coacervate layer of the composite capsule is firmly combined. As shown in Fig. 3, when the mass ratio of gelatin to gum arabic is 1 : 1, the mass ratio of TTO to cyanopropyl acrylate butyl ester is 4 : 1, and the curing time is 10 hours, the EE reaches its maximum value.

3.3 Characteristic analysis of compound capsules

3.3.1 Micromorphology and microstructure. As can be seen from Fig. 4(a), the surface shape of the unoptimized composite capsule is irregular, and there are large depressions, and the whole is irregular. Under the condition of 2000× magnification, it can be seen that the capsule is an irregular flake, which may be

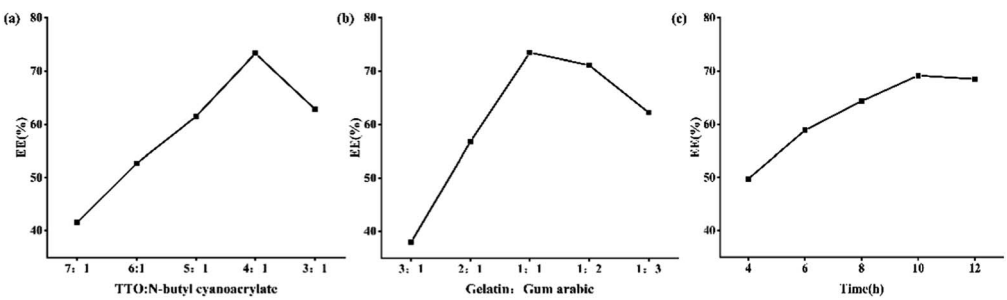

Fig. 2 Effects of ratio of TTO to n-butyl cyanoacrylate (a), mass ratio of gelatin to gum arabic (b) and curing time (c) on EE.

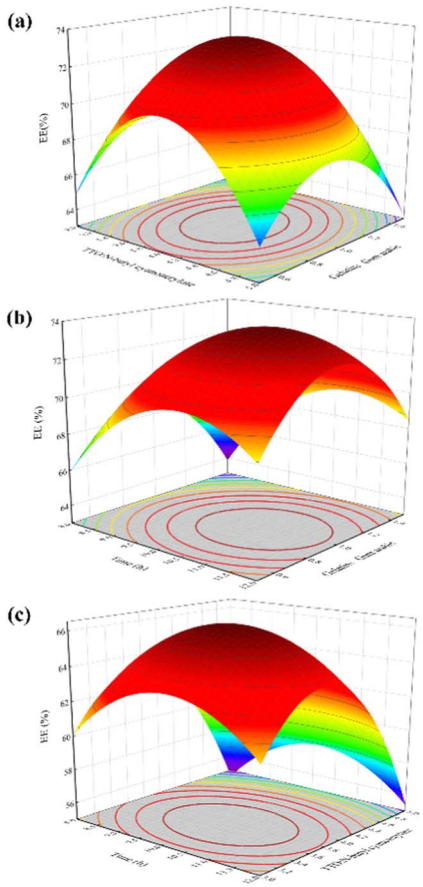

Fig. 3 Contour plot of response surface methodology: mass ratio of gelatin to gum arabic and mass ratio of TTO to cyanopropyl acrylate butyl ester (a), curing time and mass ratio of gelatin to gum arabic (b), and curing time and mass ratio of TTO to cyanopropyl acrylate butyl ester (c).

formed by the rupture of the capsule after lyophilization due to insufficient stability. In Fig. 4(b), it can be seen that the optimized composite capsule is spherical in shape with a smooth surface and a slight depression, which may be due to drying, and the gum arabic has a slight collapse.[38] At a magnification of 2000×, it can be seen that there is some aggregation in the capsule, the whole is relatively intact, and there is no rupture.

3.3.2 Particle size analysis. The particle size distribution of TTO composite capsules is observed in Fig. 5. The image displays the distribution of TTO composite capsule quantities. The results show that the particle size of the composite capsules is 5–12.8 μm, and the average particle size is 10.51 μm. The size distribution of the capsules is in a narrow range, which indicates that the size distribution of the composite capsules prepared under the optimal conditions is uniform. The smaller particle size is more conducive to the attachment of the capsule to the skin surface and meets the particle size requirements of cosmetics.

3.3.3 Fourier transform infrared spectroscopy (FT-IR) analysis. Fig. 6 shows the infrared spectra of TTO, *n*-butyl cyanoacrylate, gum arabic, and a mixture of gelatin and gum arabic, gelatin and composite microcapsules, respectively. The absorption spectrum between 3373 and 3455 cm^{-1} is the N–H stretching of amine and amide groups visible in the wall material (gelatin). In addition, the peaks between 3349 and 3344 cm^{-1} observed in the condensate correspond to gelatin polymer molecules due to the existence of amino groups (N–H stretching). The intensity of the peak is related to the amount of components used in the combination. The absorbance of functional groups in the characteristic region can be used as evidence of the existence of these groups in the molecular structure.[39]

Gum arabic is a polysaccharide containing a free carboxyl group (O–H), and its absorption spectrum ranges from 2500 to

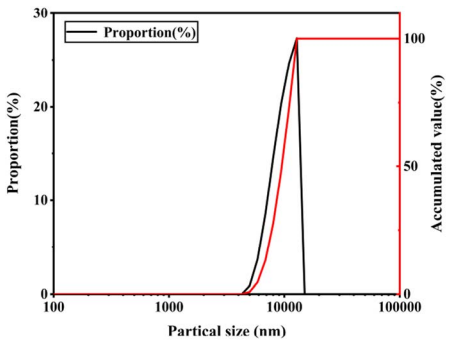

Fig. 5 Particle size distribution of TTO composite microcapsules.

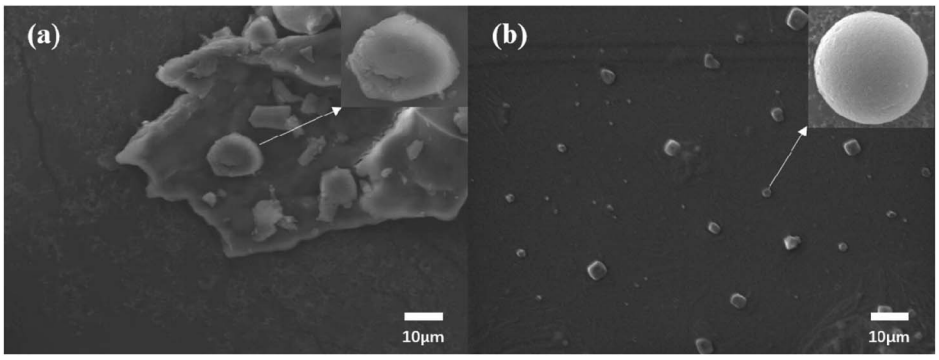

Fig. 4 (a) Scanning images of microcapsules without optimization (magnification 2000×, 6000×) and (b) scanning images of microcapsules after condition optimization (2000×, 6000×).

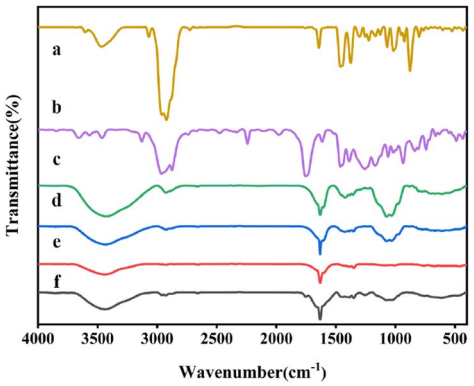

Fig. 6 FT-IR spectra of TTO (a), *n*-butyl cyanoacrylate (b), gum arabic (c), gelatin mixed with gum arabic (d), gelatin (e) and composite capsule (f).

3300 cm^{-1}, with a negatively charged molecule attached. The peak between 2921 and 2937 cm^{-1} of the condensate is due to the strong and extensive O–H stretching, which can be the free carboxyl group in gum arabic.[40] In addition, the characteristics of the amide peak can be seen at 1452 cm^{-1} in the microcapsule spectrum, which also shows a moderate C–H bending appearance. Aromatic compounds also exist in the sample formula, and the peak at 1746–1747 cm^{-1} indicates C–H bending. Through the experiment of Fourier transform infrared spectroscopy, it was confirmed that the materials of the coacervate were not simply physically mixed, and the disappearance of the TTO seal also confirmed that TTO was coated in the capsule.

3.3.4 Thermogravimetric analysis (TGA). As shown in Fig. 7, the composite capsule has a noticeable weight loss stage, and the weight loss rate is about 6.44% from 30 to 136 °C, indicating that the capsule has high volatility and can be evaporated at low temperatures. This result agrees with the previous research,[41] and the compound capsule of TTO has three stages of weight loss. In the first stage, from 136 to 198 °C, the weight loss rate is about 6.67%, in which TTO permeates from microcapsules through gasification.[42] In the second stage, from 198 to 370 °C, the weight loss rate is about 59.5%. The increase of internal pressure in this stage leads to the rupture of microcapsules and the volatilization of TTO, which is the same as the research of X. Yang *et al.*[43] In the third stage, from 370 to 600 °C, the weight loss rate is about 13.77%. At this stage, the weight loss is primarily caused by the thermal decomposition of the microcapsule shell into ash. Based on the above results, we can conclude that microencapsulation can improve the thermal stability of TTO, which may be due to the thermal resistance effect of the microcapsule shell, and the composite capsule has an excellent protective effect on TTO.[44]

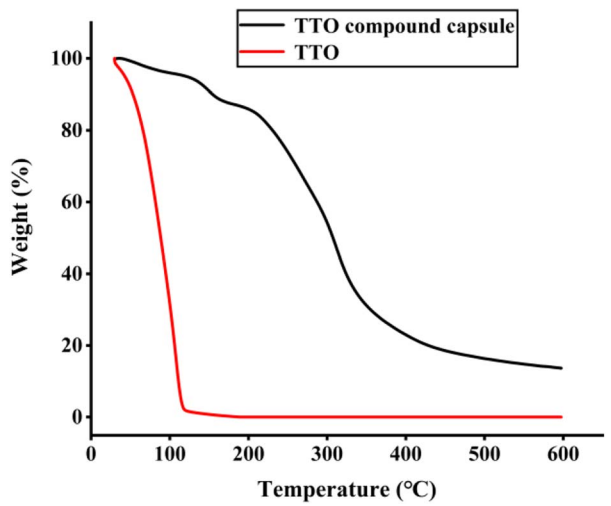

Fig. 7 Thermogravimetric analysis of TTO and TTO composite microcapsules.

3.4 Rheological property determination

Fig. 8 (a) shows the shear rate and viscosity of capsules containing *n*-butyl cyanoacrylate as a function of common complexation coagulation. As can be seen from the figure, the viscosity of the microcapsules does not change much after the addition of *n*-butyl cyanoacrylate, and the newly formed film has little effect on the viscosity of the original cohesive layer. With the increase of shear rate, the apparent viscosity decreases, and shear thinning appears, showing the characteristics of a pseudoplastic fluid caused by external force. The conformation of polymer chains in the cohesive layer is required to change.[45,46] At the same time, the polymer chains have relaxation characteristics, and the forced conformation can be wholly or partially recovered. When the shear rate is low, the molecular conformation changes slowly, and there is adequate time to recover. When the shear rate increases, the molecular conformation changes greatly, and the molecular chains cannot recover in time, which makes the polymer chains move along the direction of fluid flow. During this period, hydrogen bonds disappear, and the force decreases, showing a viscosity trend decreasing with the increase of shear rate.[47,48] However, the viscosity of microcapsules added with *n*-butyl cyanoacrylate will decrease more obviously because their condensed layer is thinner than that of ordinary microcapsules.

As presented in Fig. 8(b) and (c), the dynamic moduli of normal condensed microcapsules and those added with *n*-butyl cyanoacrylate are measured, respectively. The elastic modulus of normal condensed microcapsules is equal to the loss modulus, showing high viscosity. With the increase of angular frequency, the elastic modulus is progressively greater than the loss modulus, showing that the elasticity is greater than the viscosity.[49–52] The composite capsules added with *n*-butyl cyanoacrylate show stronger elasticity than the normal condensed capsules. Moreover, the storage modulus of the composite capsules is higher than the loss modulus at any frequency, indicating that the elastic component is the main contributor to viscoelasticity.

3.5 Volatile compound analysis

As shown in Fig. 9, TTO and TTO composite capsules have the same characteristic peaks, indicating that the main components of TTO have not changed before and after encapsulation. Therefore, the encapsulation of TTO does not affect its

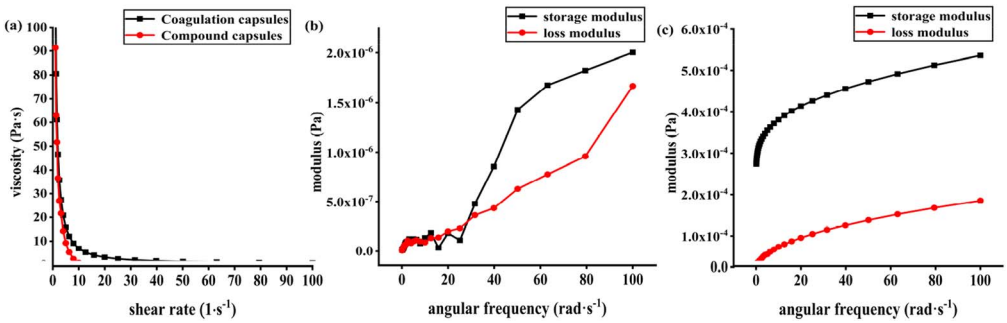

Fig. 8 Apparent viscosity of composite microcapsules (a), and storage modulus and loss modulus of common complex coacervated microcapsules (b) and composite microcapsules (c).

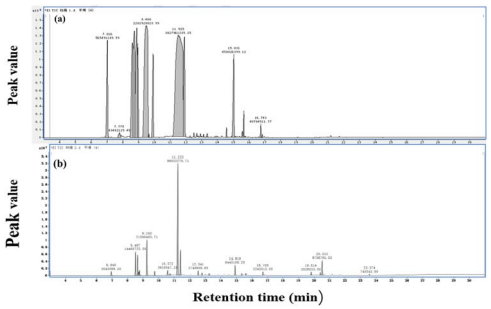

Fig. 9 Total ion chromatogram of TTO (a) and TTO composite microcapsule (b).

performance, which lays a good foundation for applying TTO composite capsules.

3.6 Stability study

In this study, a key function of the composite capsule is to serve as a transport carrier for the core material. For example, in a permeable environment, we used a solution of sodium dodecyl sulfate as an anionic surfactant to compare the stability of TTO coagulated capsules and TTO composite capsules.[16] As shown in Fig. 10, after 15 h, the composite capsules expanded significantly, and the core–shell structure decomposed, and thus released TTO. In contrast, the degree of expansion of the coagulated capsules was lower. Fig. 10(e) indicates that the TTO concentration in the solution of coagulated capsules was higher than that in the composite capsules. The results indicate that under permeable conditions, the stability of the composite capsules is better.

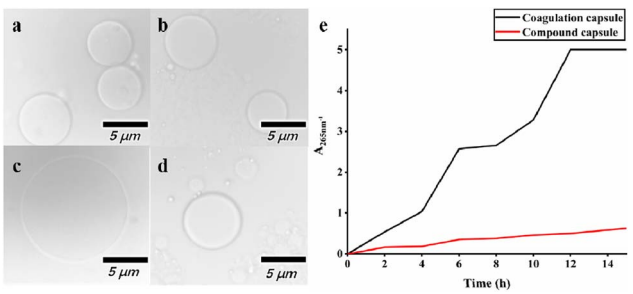

Fig. 10 The morphology of TTO condensed capsules immediately after being added to the surfactant solution (a) and 15 hours after addition (c), and the morphology of TTO composite capsules immediately after being added to the surfactant solution (b) and 15 hours after addition (d) were observed. The TTO content in the surfactant solution was determined *via* UV spectrophotometry within 15 hours (e).

3.7 *In vitro* release studies of composite microcapsules

Fig. 11 presents the release curves for TTO cohesive capsules and TTO composite capsules at human body temperature (37 °C) over a period of 15 days, along with the content of TTO released from the system. It can be observed that with the passage of time, both types of capsules gradually release increasing amounts of TTO. Notably, the cohesive capsules exhibit a burst release behavior at the beginning, followed by a gradual slowdown in the release rate, whereas the composite capsules maintain a more stable release throughout the process with a slight deceleration in rate. The results indicate that both cohesive and composite capsules have a controlled release effect on TTO, with the composite capsules showing superior control release capabilities compared to the cohesive capsules.

Fig. 12 simulates the release behavior of TTO in coagulated capsules and composite capsules under the conditions of 37 °C and pH 5.5 using four kinetic models (zero-order, first-order, Higuchi, and Peppas). Table 1 presents the release kinetic parameters of coagulated capsules and composite capsules. The model that best describes the release rate of oil from the cohesive capsules is first-order, and for the composite capsules, it is Peppas. The correlation is statistically significant.

3.8 Determination of antioxidant properties

DPPH is commonly used to detect the antioxidant capacity of active substances and can be used to estimate the clearance rate of aromatic free radicals. The ABTS detection method is also widely used, and the two methods can be combined to evaluate antioxidant activity and antioxidant capacity. Fig. 13 illustrates the variation in the scavenging ability of TTO, TTO encapsulated capsules, and TTO composite capsules on DPPH (a) and ABTS (b) free radicals over a period of 15 days. On day 0, TTO exhibited the highest activity in scavenging DPPH and ABTS

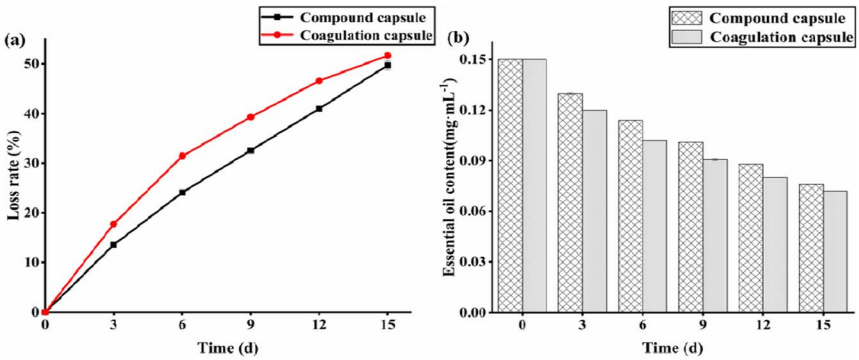

Fig. 11 Release of TTO from coacervate capsules and composite capsules under human skin conditions (37 °C, pH 5.5).

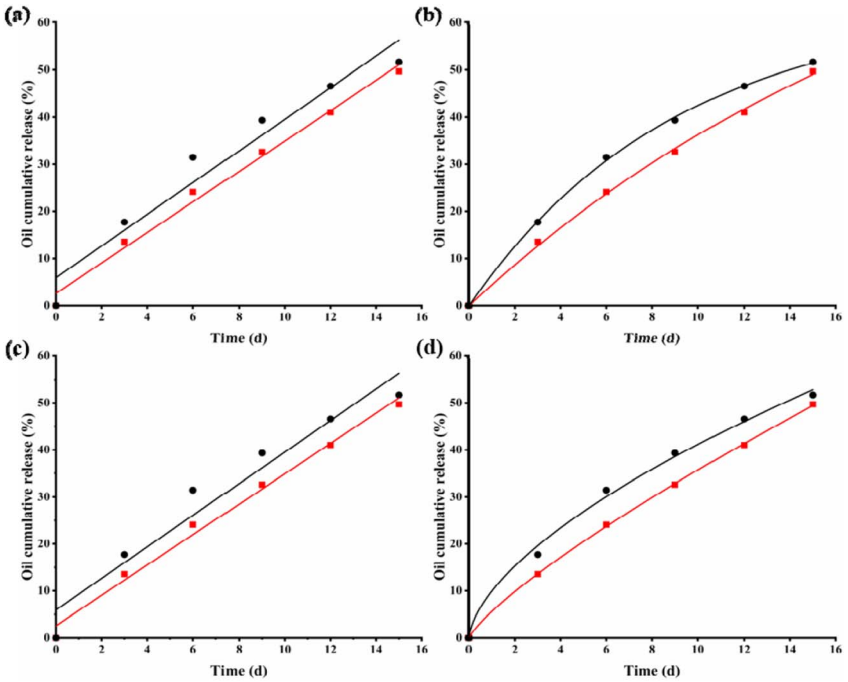

Fig. 12 Four kinetic models, zero-order (a), first-order (b), Higuchi (c), and Peppas (d), were used to fit the release behavior of TTO gel capsules and TTO composite capsules.

Table 1 Kinetic release parameters of TTO cohesive capsules and TTO composite capsules under different kinetic models

Mathematical models	Coagulation capsules	Compound capsules
Zero order	$Mt = 3.36x + 5.93$ ($R^2 = 0.93$)	$Mt = 3.23x + 2.58$ ($R^2 = 0.98$)
First order	$Mt = 63.69(1 - e^{-0.11})$ ($R^2 = 0.99$)	$Mt = 98.89(1 - e^{-0.046})$ ($R^2 = 0.98$)
Higuchi	$Mt = 6.72x^{0.5} + 5.93$ ($R^2 = 0.93$)	$Mt = 6.46x^{0.5} + 2.58$ ($R^2 = 0.98$)
Peppas	$Mt = 9.97x^{0.62}$ ($R^2 = 0.98$)	$Mt = 5.64x^{0.8}$ ($R^2 = 0.99$)

radicals, followed by TTO encapsulated beads, with TTO composite capsules showing the least activity. Throughout the storage period, the antioxidant capacity of TTO composite capsules declined the slowest, while that of TTO declined the fastest. By the 15th day of storage, the TTO composite capsules had a higher rate of scavenging for both types of free radicals compared to the TTO encapsulated beads.

The primary reason is that the level of antioxidant capacity depends on the amount of active substances in the Tea Tree Oil (TTO) within the system, meaning that the more TTO released, the stronger the antioxidant capacity. In the control group with pure TTO added to the culture medium, the initial high concentration of TTO resulted in strong antioxidant capacity. However, due to the inherent instability of essential oils, which are prone to

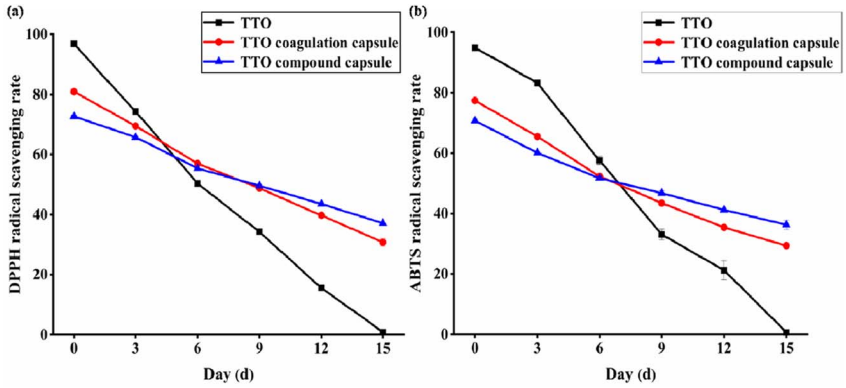

Fig. 13 Analysis of antioxidant properties: (a) DPPH radical scavenging rate; (b) ABTS radical scavenging rate.

evaporation and oxidation, the TTO content in the system decreased, leading to a rapid weakening of antioxidant capacity. In the case of TTO encapsulated beads and TTO composite capsules, the burst release of the encapsulated beads at the start resulted in a higher rate of free radical elimination than the composite capsules in the early stages of the antioxidant test. However, as the release rate of the encapsulated beads diminished over time and fell below that of the composite capsules, combined with the loss of TTO due to oxidation and evaporation, the antioxidant capacity of the encapsulated beads was lower in the later stages compared to the composite capsules. Therefore, compared to TTO encapsulated beads, the composite capsules achieved a more stable and long-lasting antioxidant effect.

4 Conclusions

In this study, the composite microcapsules were prepared by combining the composite coagulation method and the *in situ* polymerization method, and the EE of the optimized capsules was 74%. The optimized microcapsules were observed to be spherical in morphology, with a smooth surface and no cracks or cavities. Microencapsulation effectively improves the thermal stability of TTO. The results show that combining the two methods improves the mechanical properties of the two-layer membrane compared with the condensed capsule, which can maintain good stability in a certain harsh environment, has good slow-release performance, and maintains long-term stable antioxidant capacity. Therefore, TTO complex capsules have the potential to expand the application prospects of TTO in the field of cosmetics.

Conflicts of interest

The authors declare no competing financial interest.

Acknowledgements

We gratefully acknowledge the support of the Heilongjiang Province Key Research and Development Plan Project (JD22A016), Heilongjiang Province "Double first-class" discipline collaborative innovation achievement construction project (LJGXCG2022-126), Basic Scientific Research Project for Heilongjiang Provincial Colleges and Universities (2022-KYYWF-0609), Heilongjiang Provincial Key Laboratory of New Drug Development and Pharmacotoxicological Evaluation Open Fund Project (kfkt2023-09), Heilongjiang Huahao Testing Technology Service Co., LTD.

References

1 H. Li, Y. Ma, Z. Li, Y. Cui and H. Wang, *Compos. Sci. Technol.*, 2018, **164**, 120–128.
2 S. Eyupoglu, D. Kut, A. O. Girisgin, C. Eyupoglu, M. Ozuicli, H. Dayioglu, M. Civan and L. Aydin, *Text. Res. J.*, 2018, **89**, 1417–1435.
3 B. Peña, C. Panisello, G. Aresté, R. Garcia-Valls and T. Gumí, *Chem. Eng. J.*, 2012, **179**, 394–403.
4 Q. Xu, R. Qiu, Z. Bai, J. Ma, Q. Fan, Y. Li, S. Taha, Z. Ramzan and J. Li, *J. Appl. Polym. Sci.*, 2021, **138**, 51217.
5 M. A. Hernandez-Fernandez, S. Garcia-Pinilla, O. I. Ocampo-Salinas, G. F. Gutierrez-Lopez, H. Hernandez-Sanchez, M. Cornejo-Mazon, M. J. Perea-Flores and G. Davila-Ortiz, *Foods*, 2020, **9**, 1375.
6 S. J. Calva-Estrada, M. R. Mendoza, O. García, V. M. Jiménez-Fernández and M. Jiménez, *Powder Technol.*, 2018, **323**, 416–423.
7 H. S. Elshafie and I. Camele, *BioMed Res. Int.*, 2017, **2017**, 9268468.
8 N. Lourith and M. Kanlayavattanakul, *Sustainable Chem. Pharm.*, 2023, **32**, 101005.
9 P. Borotova, L. Galovicova, N. L. Vukovic, M. Vukic, E. Tvrda and M. Kacaniova, *Plants*, 2022, **11**, 558.
10 X. Liu, H. Deng, Q. Xu, K. Luo, J. Zhou, W. Gao, Z. Wang, H. Zhang and X. Zhou, *Aquac. Rep.*, 2022, **27**, 101380.
11 L. M. Devi, A. B. Das and L. S. Badwaik, *Int. J. Biol. Macromol.*, 2023, **235**, 123896.
12 Y. Li, J. Liu, X. He, D. Kong, C. Zhou, H. Wu, Z. Yang, Z. Yang and Y. Hu, *Macromol. Mater. Eng.*, 2020, **305**, 1900851.
13 W. L. Liu, Z. B. Xiao, G. Y. Zhu, R. J. Zhou, E. Q. Wang and Y. W. Niu, *Appl. Mech. Mater.*, 2013, **477–478**, 1229–1233.
14 J. D. Ogilvie-Battersby, R. Nagarajan, R. Mosurkal and N. Orbey, *Colloids Surf., A*, 2022, **640**, 128494.
15 H. H. Dai, X. D. Li, A. C. Wei, X. D. Wang and D. Y. Wang, *J. Oleo Sci.*, 2020, **69**, 685–692.

16 G. Dardelle, M. Jacquemond and P. Erni, *Adv. Mater.*, 2017, **29**, 1606099.
17 Y. Liu, W. Cao, J. Wang, L. Zhang, Y. Yang, M. Liu, H. Wang and S. Wang, *J. Food Sci.*, 2022, **87**, 5017–5028.
18 Y. Zhao, H. Li, Y. Wang, Z. Zhang and Q. Wang, *Int. J. Biol. Macromol.*, 2023, **249**, 124776.
19 P. Kaushik, K. Rawat, V. K. Aswal, J. Kohlbrecher and H. B. Bohidar, *Carbohydr. Polym.*, 2019, **224**, 115150.
20 M. S. Mesiha, M. B. Sidhom and B. Fasipe, *Int. J. Pharm.*, 2005, **288**, 289–293.
21 J. Liu, C. Liu, Y. Liu, M. Chen, Y. Hu and Z. Yang, *Colloids Surf., B*, 2013, **109**, 103–108.
22 S. Sarkar and B. Kim, *Polym. Compos.*, 2016, **39**, 636–644.
23 H. Zhang, Y. Bai and F. Cheng, *Constr. Build. Mater.*, 2018, **187**, 138–148.
24 R. S. Samakradhamrongthai, P. Thakeow Angeli, P. Kopermsub and N. Utama-Ang, *Carbohydr. Polym.*, 2019, **226**, 115262.
25 R. J. Holl and R. P. Chambers, *J. Microencapsulation*, 2002, **19**, 699–724.
26 Y. Jiang, K. Zang, J. Sun, J. Chandrapala, C. Brennan, M. Majzoobi and X. A. Zeng, *Food Res. Int.*, 2023, **172**, 113135.
27 A. Senthilkumar, A. Thangamani, K. Karthishwaran and A. J. Cheruth, *S. Afr. J. Bot.*, 2020, **129**, 100–105.
28 A. A. N. Gunny, S. J. Leem, M. M. Z. Makhtar, N. I. Zainuddin, M. H. Mohd Roslim, R. H. Raja Hashim, K. Pusphanathan, M. R. Siddiqui, M. Alam and M. Rafatullah, *Polymers*, 2023, **15**, 2722.
29 P. A. Loyeau, M. J. Spotti, N. L. Vanden Braber, Y. E. Rossi, M. A. Montenegro, G. Vinderola and C. R. Carrara, *Food Hydrocolloids*, 2018, **85**, 129–135.
30 H. H. Wang, M. Y. Li, Z. Y. Dong, T. H. Zhang and Q. Y. Yu, *Foods*, 2021, **10**, 2268.
31 Y. P. Timilsena, T. O. Akanbi, N. Khalid, B. Adhikari and C. J. Barrow, *Int. J. Biol. Macromol.*, 2019, **121**, 1276–1286.
32 T. Ma, H. Zhao, J. Wang and B. Sun, *Food Hydrocolloids*, 2019, **87**, 637–643.
33 C. Gross-Heitfeld, J. Linders, R. Appel, F. Selbach and C. Mayer, *J. Phys. Chem. B*, 2014, **118**, 4932–4939.
34 N. Ballard, S. Hamzehlou, F. Ruiperez and J. M. Asua, *Macromol. Rapid Commun.*, 2016, **37**, 1364–1368.
35 P. H. M. Marfil, B. B. Paulo, I. D. Alvim and V. R. Nicoletti, *J. Food Process Eng.*, 2018, **41**, e12673.
36 J. U. Ha, Y. J. Hwang, S. K. Jeoung, P. C. Lee, S. Y. Kim, J. K. Park, J. T. Kim and J. H. Yeom, *J. Appl. Polym. Sci.*, 2019, **136**, 47499.
37 Q. Guo, S. Li, G. Du, H. Chen, X. Yan, S. Chang, T. Yue and Y. Yuan, *LWT*, 2022, **165**, 113683.
38 M. Chen, J. Liu, Y. Liu, C. Guo, Z. Yang and H. Wu, *RSC Adv.*, 2015, **5**, 14522–14530.
39 B. Ocak, *Environ. Sci. Pollut. Res. Int.*, 2020, **27**, 42727–42737.
40 C. Cai, R. Ma, M. Duan and D. Lu, *RSC Adv.*, 2019, **9**, 19740–19747.
41 Z.-J. Zhang, N. Li, H.-Z. Li, X.-J. Li, J.-M. Cao, G.-P. Zhang and D.-L. He, *Ind. Crops Prod.*, 2018, **112**, 660–667.
42 F. M. Bezerra, M. Lis, Ó. G. Carmona, C. G. Carmona, M. P. Moisés, G. M. Zanin and F. F. Moraes, *Powder Technol.*, 2019, **343**, 775–782.
43 X. Yang, N. Gao, L. Hu, J. Li and Y. Sun, *J. Food Eng.*, 2015, **161**, 87–93.
44 Z. Yang, Z. Peng, J. Li, S. Li, L. Kong, P. Li and Q. Wang, *Food Chem.*, 2014, **145**, 272–277.
45 J. Sprakel, S. B. Lindstrom, T. E. Kodger and D. A. Weitz, *Phys. Rev. Lett.*, 2011, **106**, 248303.
46 T. Divoux, V. Grenard and S. Manneville, *Phys. Rev. Lett.*, 2013, **110**, 018304.
47 A. P. Dhand, R. Poling-Skutvik and C. O. Osuji, *Soft Matter*, 2021, **17**, 4517–4524.
48 R. Radhakrishnan, T. Divoux, S. Manneville and S. M. Fielding, *Soft Matter*, 2017, **13**, 1834–1852.
49 W. Xiong, C. Ren, W. Jin, J. Tian, Y. Wang, B. R. Shah, J. Li and B. Li, *Food Hydrocolloids*, 2016, **61**, 895–902.
50 Q. Ru, Y. Wang, J. Lee, Y. Ding and Q. Huang, *Carbohydr. Polym.*, 2012, **88**, 838–846.
51 M. Raei, A. Rafe and F. Shahidi, *J. Food Eng.*, 2018, **228**, 25–31.
52 D. Dong and B. Cui, *J. Food Process Eng.*, 2019, **42**, e13169.